Supporting Information for:

Architectural Engineering of Rod-Coil Compatibilizers for Producing Mechanically and Thermally Stable Polymer Solar Cells

Hyeong Jun Kim,[†] Jae-Han Kim,[‡] Ji-Ho Ryu,[§] Youngkwon Kim,[†] Hyunbum Kang, [†] Won Bo Lee,[§]

Taek-Soo Kim[*‡] and Bumjoon J. Kim*[*†]*

Table of Contents

E-mail: bumjoonkim@kaist.ac.kr, tskim1@kaist.ac.kr

Synthesis and Characterizations

General: Unless otherwise noted, commercially available reagents were used without further purifications. The progress of chemical reactions was checked with thin-layer chromatography (TLC) analysis using Merck silica gel 60 F254 pre-coated plates (0.25 mm) with a fluorescent indicator and was visualized with UV light (254 and 365 nm). Column chromatography was carried out on Merck silica gel 60 (230-400 mesh). All ^{1}H-NMR spectra were recorded at 500 MHz, using $CDCl_3$ as a solvent. The chemical shifts of all ^{1}H-NMR spectra are referenced to the residual signal of $CDCl_3$ (δ 7.26 ppm) using Bruker 500 MHz NMR instrument.

1. Detailed Synthetic Procedure of P3HT-*g*-P2VP copolymers

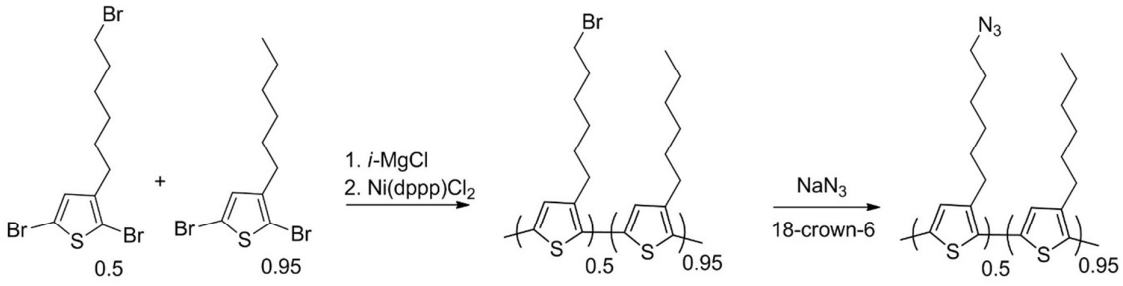

Scheme S1. Synthesis of azide-functionalized P3HT copolymers (**P3HT-alkyl-azide**)

P3HT-alkyl-azide were synthesized according to our previous reported route.[1, 2]

^{1}H NMR (500 MHz, $CDCl_3$) δ 6.98 (s, 1H), 3.28 (t, *J* = 6.5 Hz, N_3CH_2, 2H (5%)), 2.81 (t, *J* = 7.5 Hz, CH_2, 2H), 1.65-1.76 (m, CH_2, 2H), 1.40-1.50 (m, CH_2, 2H), 1.26-1.40 (m, CH_2CH_2, 4H), 0.92 (t, *J* = 6.5 Hz, CH_3, 3H (95%)).

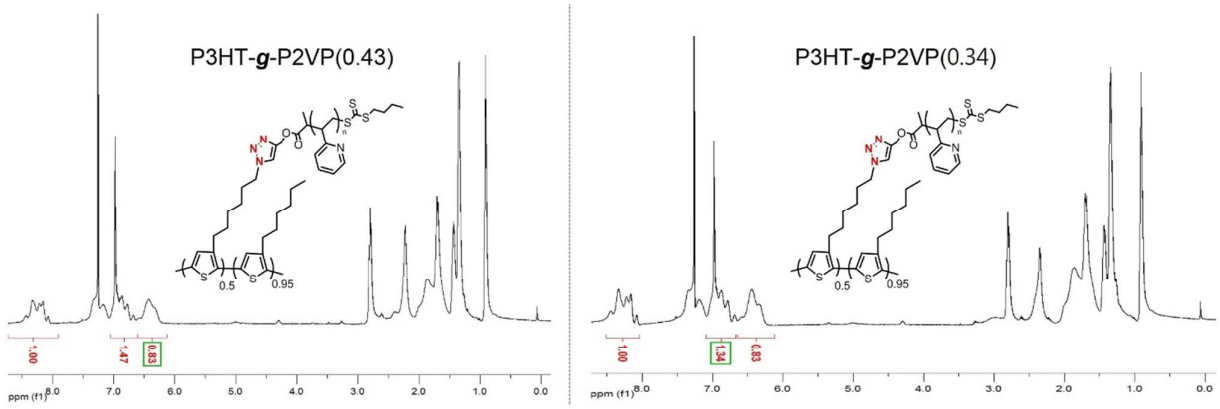

Figure S1. [1]H-NMR spectra for the P3HT-*g*-P2VP(0.43) and P3HT-*g*-P2VP(0.34) copolymers

2. Detailed Synthetic Procedure of P3HT-*b*-P2VP copolymers

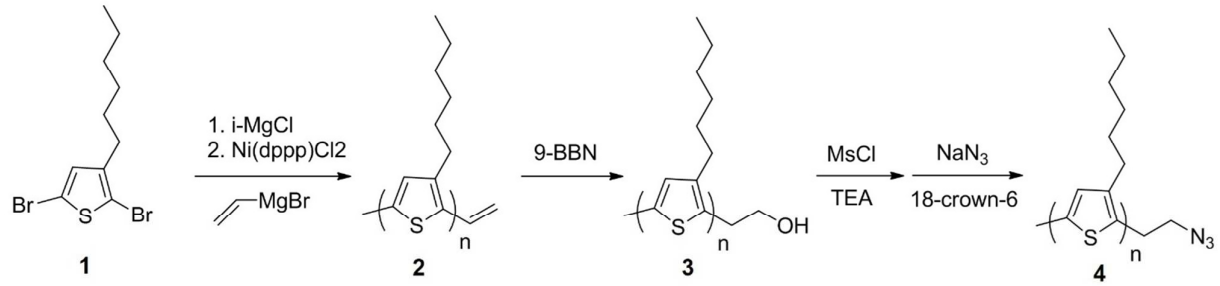

Scheme S2. Synthesis of azide-end group functionalized P3HT copolymers (**P3HT-end-azide**)

***P3HT-end-vinyl (2)*:** The 2,5-bromo-3-hexylthiophene (**1**) (2 g, 6.13 mmol) was placed in the flask under nitrogen atmosphere. Dry THF (40 ml) was added into the flask with a syringe, and the mixture was stirred at 0 °C. Isopropyl-magnesium chloride (2.0 M solution in THF, 3.01 ml, 6.02 mmol) was added and the mixture was stirred at 0 °C for 1 h. Polymerization was initiated through addition of Ni(dppp)Cl_2 suspension (37.8 mg , 0.074 mmol) in dry THF (3 ml) to the mixture and the reaction was carried out at room temperature for 30 min. The polymerization was terminated with 0.3 ml of vinyl magnesium bromide solution (1.0 M solution in THF). The reaction mixture was stirred for 15 min followed by precipitating in methanol, and the resulting precipitate was then filtered.

Oligomers and impurities in the product were removed via Soxhlet extractions with methanol (MeOH) and hexane, followed by chloroform extraction. The resulting solid was dried under vacuum to yield the product (**3**). ^{1}H NMR (500 MHz, $CDCl_3$) δ 6.98 (s, 1H), 6.61 (t, 1H), 5.52 (d, 2H), 5.13 (d, 2H), 2.80 (t, 2H), 1.66 (t, 2H), 1.35-1.41 (m, 6H), 0.91 (t, 3H).

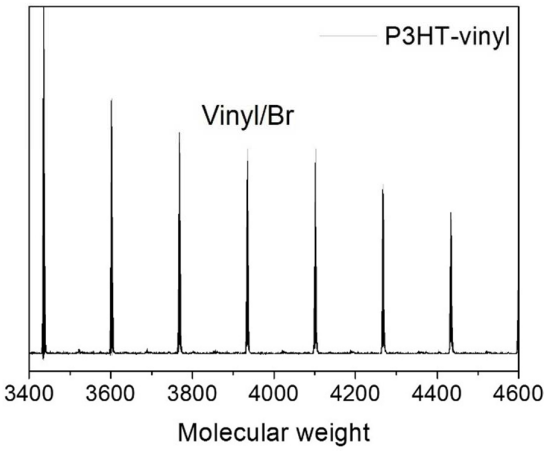

Figure S2 MALDI-TOF analysis of **P3HT-end-vinyl** polymer. Synthesized **P3HT-end-vinyl** contains very homogeneous Br/vinyl end group

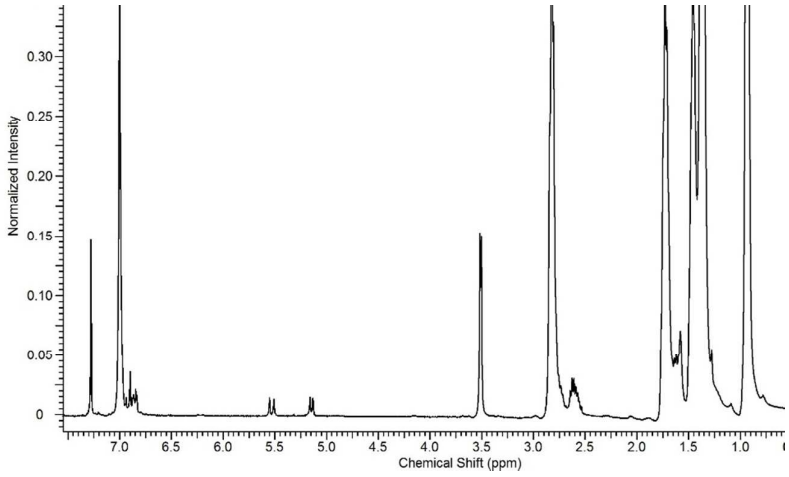

Figure S3. ^{1}H-NMR spectra for **P3HT-end-vinyl**

P3HT-end-OH ***(3)***: **P3HT-end-vinyl** ***(2)*** (1 g, 0.16 mmol,) was dissolved in fresh THF (10 mL) under nitrogen. 0.5 M solution of 9-BBN (3.2 mL, 1.6 mmol) in THF was added to mixture via a

syringe. The reaction mixture was stirred for 24 h at 40°C, at which point a 6 M solution of NaOH (1 mL) was added to the reaction flask. The reaction mixture was stirred for another 15 min (at which point the oil bath was removed). The reaction mixture was allowed to cool down to RT, followed by addition of 33% aqueous solution of hydrogen peroxide (1 mL), and the reaction was allowed to proceed for additional 24 h at 40°C. The **P3HT-end-OH (3)** was isolated by precipitation in MeOH. ^{1}H NMR (500 MHz, $CDCl_3$) δ 6.98 (s, 1H), 3.72 (t, 2H), 3.21 (t, 2H), 2.69 (t, 2H), 1.62 (t, 2H), 1.35-1.43 (m, 6H), 0.91 (d, 3H).

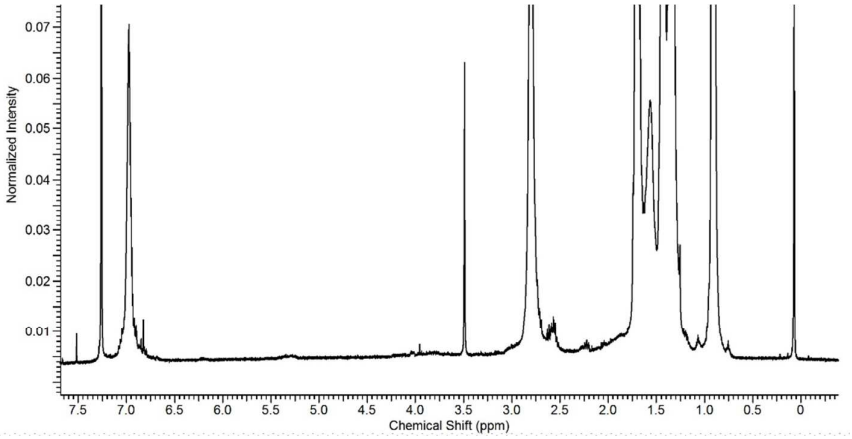

Figure S4. ^{1}H-NMR spectra for **P3HT-end-OH**

P3HT-end-azide *(4):* the **P3HT-end-OH (3)** (1 g, 0.16 mmol) was dissolved in fresh THF (40 mL) under nitrogen. Triethylamine (0.18 ml,1.28 mmol) was added, and then methanesulfonyl chloride (0.12 ml, 1.6 mmol) was added to the flask and the solution was stirred at room temperature for overnight. The polymer was precipitated with MeOH and then dried under vacuum. After drying under vacuum, the **mesylated P3HT** (1 g, 0.16 mmol) was dissolved in THF (40 mL). The NaN_3 (83.2 mg, 1.28 mmol) and 18-crown-6 (338.32 mg 1.28 mol) was dissolved in DMF (10 mL) and sonication was applied for 30 min to obtain homogeneous solution. DMF solution was added to THF solution and then refluxed for 8 h under nitrogen atmosphere. The polymer was precipitated with MeOH and the resulting precipitate was then filtered. Residual NaN_3 was removed via Soxhlet

extractions with MeOH for 8 h. The resulting solid was dried under vacuum to yield the product (**4**). ^{1}H NMR (500 MHz, $CDCl_3$) δ 6.98 (s, 1H), 3.72 (t, 2H), 3.28 (t, 2H), 2.69 (t, 2H), 1.62 (t, 2H), 1.35-1.43 (m, 6H), 0.91 (d, 3H).

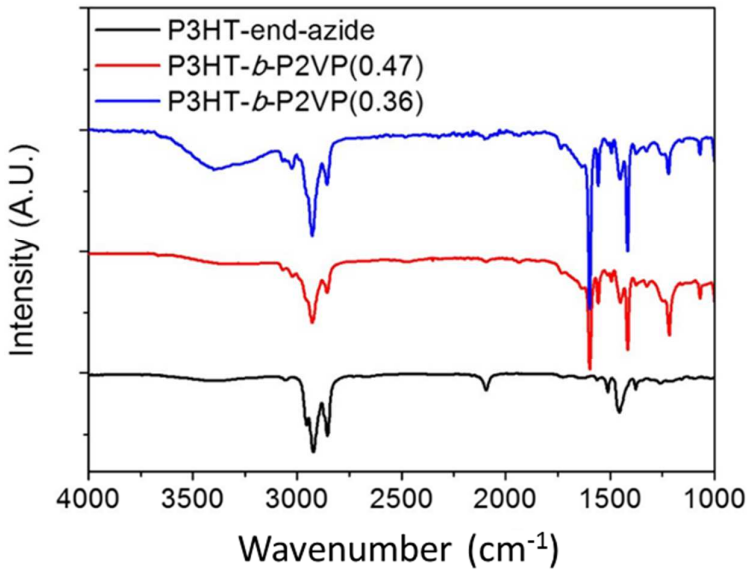

Figure S5. FT-IR spectra for **P3HT-end-azide**, P3HT-*b*-P2VP(0.47) and P3HT-*b*-P2VP(0.36). After the click reaction, the azide peak at 2100 cm^{-1} was disappeared

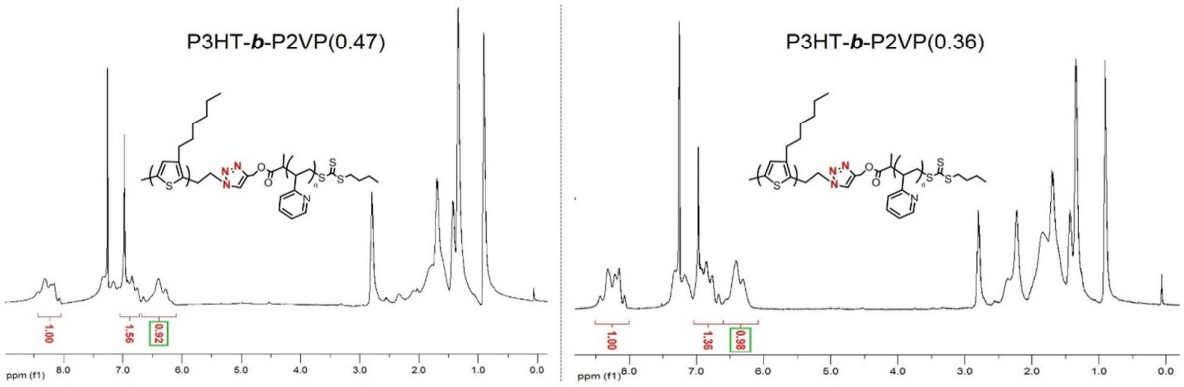

Figure S6. ^{1}H-NMR spectra for P3HT-*b*-P2VP(0.47) and P3HT-*b*-P2VP(0.36)

2. Device Performances and Characterizations

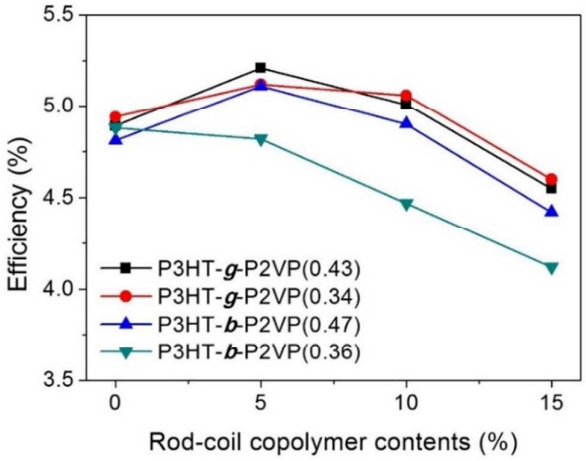

Figure S7. Initial performances of P3HT/OXCBA devices containing different weight ratios of rod-coil copolymers. The weight ratio of rod-coil copolymers to P3HT was varied from 0 to 15% with the respect to the P3HT weight in the blends

Table S1. Photovoltaic parameters of the P3HT/OXCBA device with different weight fractions of copolymers

Type	Contents (%)	V_{oc} (V)	J_{sc} (mA/cm^2)	FF	PCE (%)
P3HT-*g*-P2VP(0.43)	0	0.88	9.10	0.61	4.89
	5	0.89	9.28	0.63	5.21
	10	0.89	9.12	0.62	5.01
	15	0.88	8.93	0.58	4.55
P3HT-*g*-P2VP(0.34)	0	0.87	9.30	0.61	4.94
	5	0.88	9.19	0.64	5.12
	10	0.89	9.22	0.62	5.06
	15	0.88	8.99	0.58	4.60
P3HT-*b*-P2VP(0.47)	0	0.88	9.10	0.60	4.81
	5	0.89	9.30	0.62	5.11
	10	0.88	8.65	0.64	4.90
	15	0.88	8.76	0.57	4.42
P3HT-*b*-P2VP(0.36)	0	0.89	8.81	0.63	4.88
	5	0.89	8.50	0.63	4.82
	10	0.88	9.01	0.56	4.47
	15	0.89	8.96	0.52	4.12

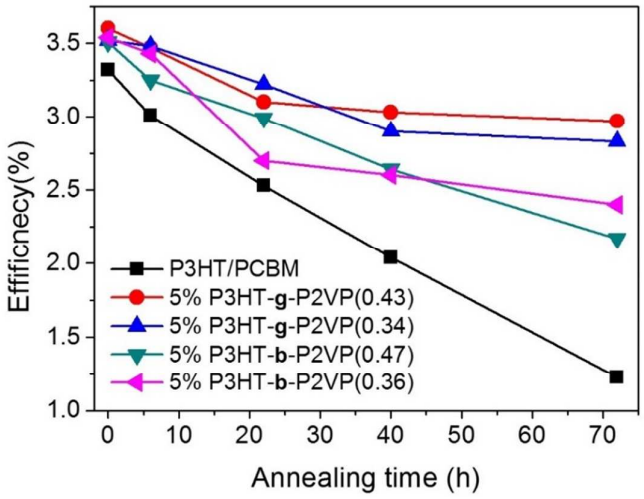

Figure S8. Efficiencies of P3HT/PCBM devices containing 5% of P3HT-*g*-P2VP(0.43), P3HT-*g*-P2VP(0.34), P3HT-*b*-P2VP(0.47), and P3HT-*b*-P2VP(0.36) during thermal annealing at 120°C

Table S2. Photovoltaic parameters of P3HT/PCBM devices including 5 mol% of different rod-coil copolymers with thermal annealing at 120°C.

	Annealing time (h)	V_{oc} (V)	J_{sc} (mA/cm^2)	FF	**PCE (%)**
P3HT/PC_{61}BM	0	0.63	8.07	0.66	**3.40**
	72	0.42	6.25	0.46	**1.23**
P3HT-***g***-P2VP(0.43)	0	0.64	8.63	0.65	**3.60**
	72	0.62	8.23	0.58	**2.97**
P3HT-***g***-P2VP(0.34)	0	0.64	8.77	0.63	**3.53**
	72	0.61	7.54	0.61	**2.83**
P3HT-***b***-P2VP(0.47)	0	0.65	8.46	0.64	**3.51**
	72	0.63	6.68	0.52	**2.17**
P3HT-***b***-P2VP(0.36)	0	0.65	8.51	0.64	**3.54**
	72	0.60	7.40	0.54	**2.39**

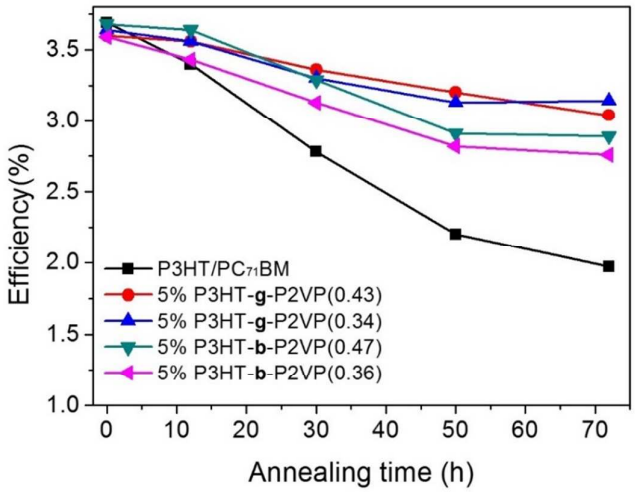

Figure S9. Efficiencies of P3HT/$PC_{71}BM$ devices containing 5% of P3HT-g-P2VP (0.43), P3HT-g-P2VP(0.34), P3HT-b-P2VP(0.47) and P3HT-b-P2VP(0.36) during thermal annealing at 120°C

Table S3. Photovoltaic parameters of P3HT/$PC_{71}BM$ devices including 5 mol% of different rod-coil copolymers with thermal annealing at 120°C

	Annealing time (h)	V_{oc} (V)	J_{sc} (mA/cm^2)	FF	**PCE (%)**
P3HT/$PC_{71}BM$	0	0.64	9.03	0.64	**3.69**
	72	0.55	8.33	0.44	**2.02**
P3HT-***g***-P2VP(0.43)	0	0.65	9.00	0.61	**3.60**
	72	0.62	8.63	0.57	**3.05**
P3HT-***g***-P2VP(0.34)	0	0.66	9.22	0.60	**3.64**
	72	0.62	9.11	0.56	**3.14**
P3HT-***b***-P2VP(0.47)	0	0.66	9.10	0.62	**3.68**
	72	0.61	8.49	0.56	**2.89**
P3HT-***b***-P2VP(0.36)	0	0.65	9.11	0.60	**3.59**
	72	0.60	8.86	0.52	**2.76**

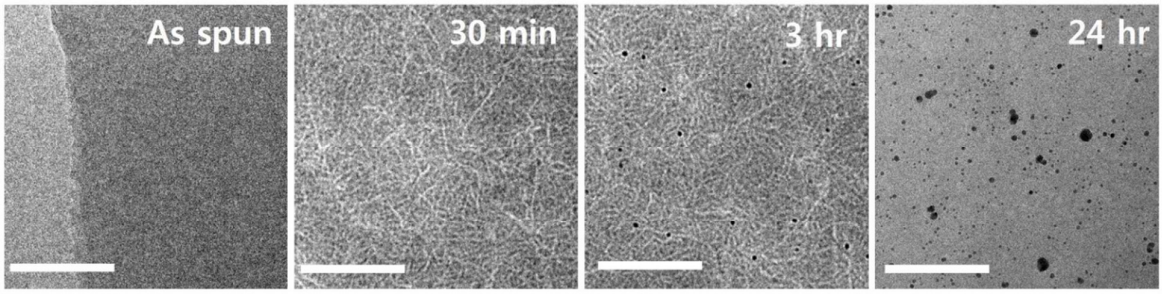

Figure S10. TEM images for the P3HT/OXCBA films as a function of the annealing time at 150^{o}C (scale bar = 200nm)

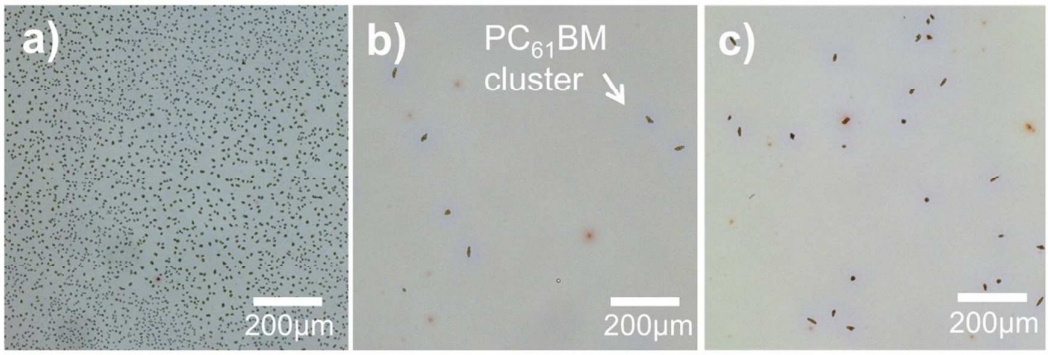

Figure S11. Optical microscopy images of the P3HT/PCBM films containing a) 0 % and 5% of b) P3HT-*g*-P2VP(0.43) and c) P3HT-*b*-P2VP(0.47) after annealing at 120 ^{o}C for 12 h. Thermal annealing induced the formation of many of overgrown PCBM crystallites that have over 20 μm in length in the P3HT/PCBM blend. In contrast, the devices with either P3HT-*g*-P2VP(0.43) or P3HT-*b*-P2VP (0.47) copolymers had significantly reduced to no dark PCBM crystals

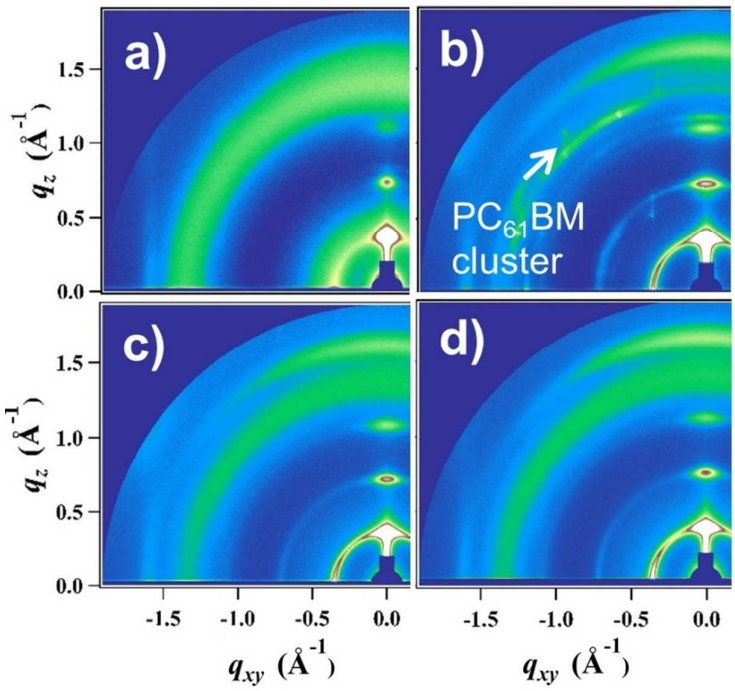

Figure S12. . GI-WAXS images of the P3HT/PCBM films a) before and b) after annealing at 120 ^{o}C for 24 h. Whereas sharp and prominent scattering peaks from PCBM aggregates were distinctly observed for the P3HT/PCBM reference device, the devices that contained 5 % of c) P3HT-*g*-P2VP(0.43) and d) P3HT-*b*-P2VP(0.47) compatibilizers exhibited very broad PCBM peaks

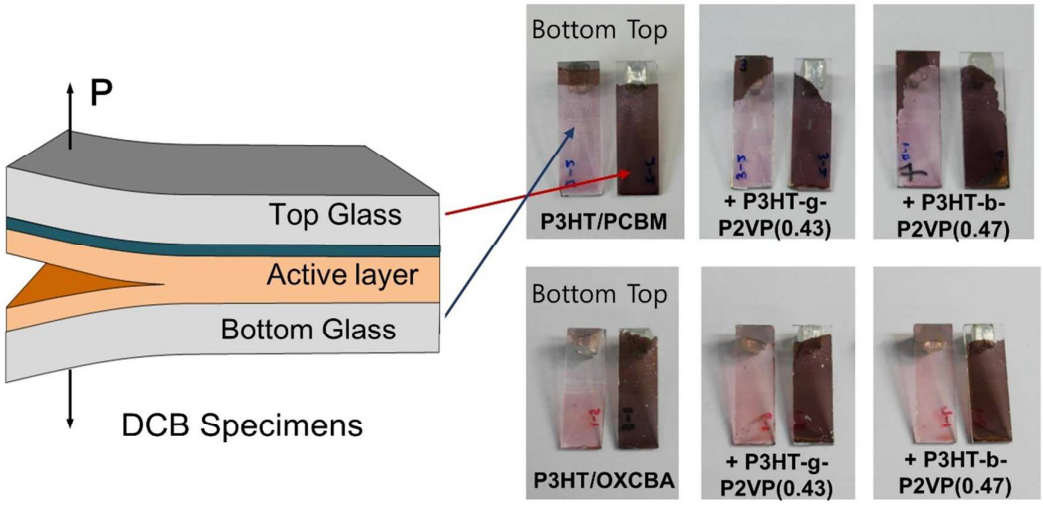

Figure S13. Specimens of BHJ films after DCB test. Cohesive failures were observed for all specimens

Preparation of TEM samples: Thin films (~ 50 nm) of P3HT/OXCBA for TEM measurement were prepared on 50 nm glass substrate with the identical condition for PSC, but cast from reduced concentration (7.5 mg/ml) in solution. Films were subsequently floated-off in distilled water and picked up with copper TEM grids. Samples were dried for 24 h under vacuum and subsequently annealed at 150^{o}C on a digital hot plate in a N_2 glove box.

GI-WAXS measurement: GI-WAXS measurements were performed on beamline 9A in the Pohang Accelerator Laboratory (South Korea). The active layers were spin coated on Si-wafer and annealed at the identical conditions for preparation of PSC devices. X-rays with a wavelength of 1.1010 Å were used. The incidence angle (~ 0.14^{o}) was carefully chosen to allow for complete X-ray penetration into the polymer film. The scattering spectra were collected as the 2D image map and that divided into a component in the plane of the substrate (q_{xy}) and a component perpendicular to the substrate (q_z).

3. Computational Simulations

Coarse-grained Bead-spring Molecular Dynamics Simulations: The potential energy of the system includes two distinct contributions.

$$U_{total} = U_{non-bond} + U_{bond}$$

The first term of total potential energy of system is non-bonded potential between each bead. To describe the polymeric liquid solution, non-bonded potential is represented by only repulsive Lennard-Jones potential, Weeks-Chandler-Andersen potential, $r_c = 2^{1/6} \cdot \sigma$.

$$U_{non-bond}(r) = \begin{cases} 4\varepsilon\left[\left(\frac{\sigma}{r}\right)^{12} - \left(\frac{\sigma}{r}\right)^{6}\right] + \varepsilon, (r \le r_c) \\ 0 \qquad\qquad\qquad , (r \ge r_c) \end{cases}$$

The bond potential energy, second term of total energy, is described by a simple pair potential of the harmonic form.

$$U_{bond} = \frac{1}{2} k_{bond}(l - l_0)$$

The coefficients k_{bond} and l_0 are parameter representing the bond strength and average bond length at equilibrium, respectively.

When system is constructed for molecular dynamics, initial configuration is usually in very high energy state due to overlaps with beads and non-optimal position of beads. We have combined energy minimization and simulated annealing to obtain minimal energy structure. Energy minimization is performed to decrease the energy state of system by removing van der Waals overlaps using steepest descent method. Then simulated annealing process is performed for position optimization, from T=560K to 380K (50τ per step), $\tau = \sigma(m/\varepsilon)^{1/2}$. Velocities of beads for trajectory of simulation are generated according to Boltzmann distribution. The simulation is executed using leap-frog stochastic dynamics in isothermal-isochoric (NVT) condition, T=373K with a time step of 0.001τ. The box dimension is $20 \times 20 \times 20\sigma^{-3}$ in the x-, y- and z-directions. We have prepared A and B homopolymer blend containing 212A homopolymer and 212 B homopolymer chains. Each homopolymer is composed of 30 beads. Compatibilizers (diblock copolymer and grafted copolymer) consist of 30 beads of A species and 30 beads of B species. In the case of the block copolymer, A block is linearly connected to B block. For the graft copolymers, two short chains composed of 15 beads are anchored to a main backbone at the interval of 10 beads. The number of compatibilizers in the system was four.

For precise comparison of interfacial width changes due to the addition of two different copolymers, interfacial width $\boldsymbol{\delta}$ is calculated by following equation (1).[3, 4]

$$\rho(d) = \frac{1}{2}\left(1 + \tanh\left[\frac{2(d - d_0)}{\delta}\right]\right) \qquad (1)$$

where $\boldsymbol{\rho}$ and $\mathbf{d_0}$ are the density fraction and position of the interface, respectively.

The interfacial tension is calculated according to the methods of modified Irving and Kirkwood equation[5] for practical purposes, which is defined by the difference between normal and lateral pressure tensor across the interface. The modified Irving and Kirkwood equation involves a spatial averaging using a smooth kernel function. The formula for the stress has been known as Hardy stress tensor. For the reducing of fluctuation, we have processed the time averaging.

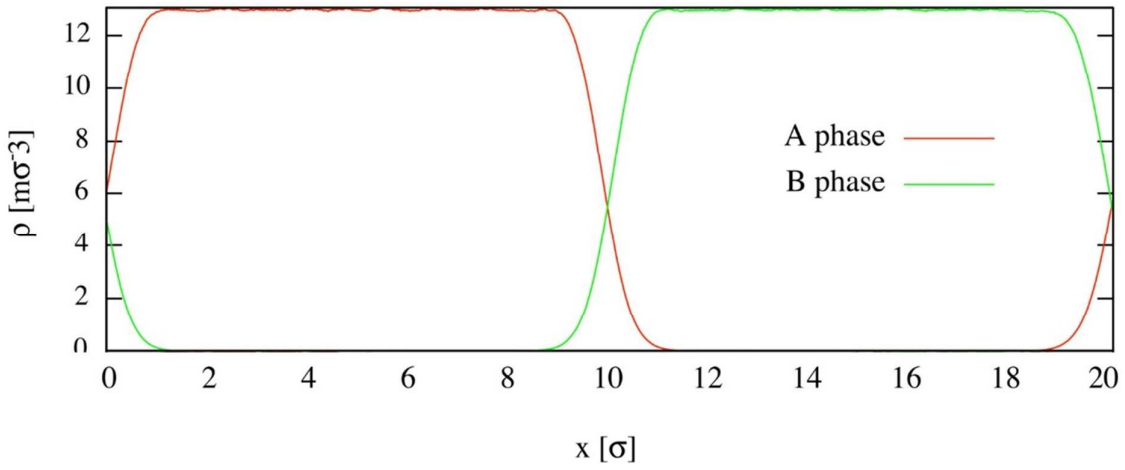

Figure S14. The density profile for immiscible A/B homopolymer bilayer blends after energy minimization and simulated annealing process were applied to obtain minimum energy structure

References

1. Kim, H. J.; Paek, K.; Yang, H.; Cho, C.-H.; Kim, J.-S.; Lee, W.; Kim, B. J. Molecular Design of "Graft" Assembly for Ordered Microphase Separation of P3HT-Based Rod–Coil Copolymers. *Macromolecules* **2013**, *46*, 8472-8478.
2. Kim, H. J.; Han, A. R.; Cho, C.-H.; Kang, H.; Cho, H.-H.; Lee, M. Y.; Fréchet, J. M. J.; Oh, J. H.; Kim, B. J. Solvent-Resistant Organic Transistors and Thermally Stable Organic Photovoltaics Based on Cross-Linkable Conjugated Polymers. *Chem. Mater.* **2011**, *24*, 215-221.
3. Kim, S. H.; Jo, W. H. A Monte Carlo Simulation of Polymer Polymer Interface in the Presence of Block Copolymer. I. Effects of the Chain Length of Block Copolymer and Interaction Energy. *J. Chem. Phys.* **1999**, *110*, 12193-12201.
4. Zhou, Y.; Long, X.-P.; Zeng, Q.-X. Dissipative Particle Dynamics Studies on the Interface of Incompatible A/B Homopolymer Blends in the Presence of Nanorods. *Polymer* **2011**, *52*, 6110-6116.
5. Irving, J. H.; Kirkwood, J. G. The Statistical Mechanical Theory of Transport Processes. 4. The Equations of Hydrodynamics. *J. Chem. Phys.* **1950**, *18*, 817-829.